The relationships between *Mycobacterium tuberculosis* MGIT time to positivity and colony forming units in sputum samples demonstrates changing bacterial phenotypes potentially reflecting the impact of chemotherapy on critical sub-populations

Ruth BOWNESS [1]*, Martin J BOEREE [2], Rob AARNOUTSE[3], Rodney DAWSON [4], Andreas DIACON [5], Chacha MANGU [6], Norbert HEINRICH [7,8], Nyanda E NTINGINYA [6], Anke KOHLENBERG [6,7], Bariki MTAFYA [6], Patrick PJ PHILLIPS [9], Andrea RACHOW [7,8], Georgette PLEMPER VAN BALEN [2], Stephen H GILLESPIE [1]

[1] School of Medicine, University of St Andrews, Fife, Scotland, KY16 9AJ, UK

[2] Radboud University Medical Center, Department of Pulmonary Diseases, Nijmegen, The Netherlands

[3] Radboud University Medical Center, Department of Clinical Pharmacy, Nijmegen, The Netherlands

[4] Radboud Division of Pulmonology, Department of Medicine and University of Cape Town Lung Institute, Cape Town, South Africa

[5] Department of Biomedical Sciences, Faculty of Medicine and Health Sciences, Stellenbosch University, Cape Town, South Africa

[6] NIMR-Mbeya Medical Research Centre, P.O.BOX 2410, Mbeya, Tanzania

[7] Department for Infectious Diseases and Tropical Medicine, University of Munich, Munich, Germany

[8] DZIF German Centre for Infection Research, Munich, Germany

[9] Medical Research Council (MRC) Clinical Trials Unit at UCL, London, UK

*Corresponding author: Ruth Bowness, School of Medicine, University of St Andrews, Fife, Scotland, KY16 9AJ, UK.

Tel: +44 1334 463564, Fax: +44 1334 463330, E-mail: rec9@st-andrews.ac.uk

Running title: Sub-populations of M.tb

Keywords: TTP, MGIT, cfu, *Mycobacterium tuberculosis,* sputum

ABSTRACT

Objectives

The relationship between colony forming units (cfu) and Mycobacterial Growth Indicator Tube (MGIT) time to positivity (TTP) is uncertain. We attempted to understand this relationship and create a mathematical model to relate these two methods of determining mycobacterial load.

Methods

Sequential bacteriological load data from clinical trials determined by MGIT and cfu was collected and mathematical models derived. All model fittings were conducted in the R statistical software environment (version 3.0.2), using the lm and nls functions.

Results

TTP showed a negative correlation with $\log_{10}$(cfu) on all 14 days of the study. There was of increasing gradient of the regression line and y-intercept as treatment progressed. There was also a trend towards an increasing gradient with higher doses of rifampicin.

Conclusions

These data suggest that there is a population of mycobacterial cells that are more numerous when detected in liquid than in solid medium. Increasing doses of rifampicin differentially kills this group of organisms. These findings support the idea that increased doses of rifampicin are more effective.

INTRODUCTION

If we are to improve the outcome of tuberculosis, it is essential that we develop shorter effective treatment regimens.[1] Late relapse is thought to result from a population of dormant cells that are relatively resistant to chemotherapy.[2] This has prompted extensive *in vitro* experiments with description of a range of dormancy models *in vitro* [3,4] and *in vivo.*[5] A number of recent publications have also postulated multiple populations of *M. tuberculosis* cells in differing states within patients with pulmonary tuberculosis although there are few studies that link the different phenotypes. This concept has arisen from the findings of early phase clinical trials that demonstrate that isoniazid has its greatest effect in the first two days.[6,7] It is known that mycobacterial cells in artificial culture accumulate lipid bodies as they enter a stationary phase, an effect that is found in all species of the genus.[8,9] Such cells may not grow on solid media unless resuscitated by the addition of resuscitation promotion factors (Rpf), first described in high GC Gram positive bacteria.[10] A number of in vitro models have described these "dormant" forms.[3,4,11,12] Wayne described these cells as non-replicating-persistent (NRP) cells.[3,13] The bacterial pheromones (Rpfs) associated with activating non-plateable cells are expressed on the surface of *M. tuberculosis* in human granulomas.[14] Importantly, it has also been recognised that in human sputum samples, on average, up to 90% of the cells at baseline are not cultured on solid medium without the addition of Rpf from spent medium.[15]

Previous studies have demonstrated that liquid media are more sensitive than solid media for culture of mycobacteria from sputum and liquid media reduces

the number of subjects with negative cultures at 8 weeks.[16] In this study we explore the relationship between matched liquid culture and colony count data from patients during the first fourteen days of treatment. We also try to detect a population of organisms that cannot be cultured on solid medium but are capable of growth in liquid medium, and determine whether the proportion of these organisms remains constant during this initial phase, and whether we are able to estimate the relationship between colony counts on solid medium and TTP.

METHODS

Patients and treatment dosage

Clinical trial data were obtained from two patient datasets. The site's local and national ethics boards approved these studies. The studies were conducted in compliance with ICH Good Clinical Practice Guidelines and the declaration of Helsinki. All patients provided written informed consent to study participation.

We primarily focused on the HIGHRIF1 trial (www.clinicaltrials.gov, NCT01392911), a multiple ascending dose study in which increasing doses of rifampicin from 10-35 mg/kg were evaluated. Adult patients were recruited in University of Cape Town Lung Institute and Stellenbosch University. They were given rifampicin mono-therapy alone for days 1-7, followed by the addition of isoniazid, pyrazinamide and ethambutol at standard doses for a further seven days. Data were obtained from a total of 68 patients: 15 patients per arm and 8 in a control arm. Sputum was collected twice at baseline (pre-treatment) and

then at days 1, 2, 3, 4, 5, 6, 7, 9, 14 during treatment. At each visit, sputum was collected overnight (16:00hr until 08:00 the following morning inclusive. This dataset was randomly split in two, where the first half was used as a training dataset, and the second as a test dataset.

A second dataset was used to test the observations and models that were created. The data were collected from the Mbeya site of the OEBA (Observation of Early Bactericidal Activity) (Pan African Clinical Trials Registry (pactr.org) under PACTR201209000394102). A total of 23 eligible adults (male and female aged 18-65 inclusive), with newly diagnosed, sputum smear positive, drug susceptible pulmonary tuberculosis were enrolled in the study at the Tanzanian National Institute for Medical Research - Mbeya Medical Research Centre. Individuals were hospitalised for up to 17 days at the OEBA unit and received standard isoniazid, rifampicin, pyrazinamide and ethambutol (HRZE) anti-tuberculosis treatment followed by standard treatment according to Tanzanian national guidelines. Sputum was collected twice at baseline (pre-treatment) and then at days 2, 4, 5, 7, 10, 14 (T2-T14) during treatment. At each visit, sputum was collected overnight (16:00hr until 08:00 the following morning inclusive.

Bacteriological methods

Prospective sequential patient sputum samples were inoculated into the Mycobacterial Growth Indicator Tube (MGIT; BBL Becton Dickinson Microbiology Systems) and TTP recorded. In parallel the colony forming units were enumerated using serial dilution on selective Middlebrook 7H10 medium as described previously.[17]

Statistical methods

In this paper, the relationship between TTP and $\log_{10}$(cfu) was examined. Although some authors have previously used log-transformed TTP when analysing the relationship with $\log_{10}$(cfu),[18] we found that it resulted in a poorer model fit and hence we chose to explore the relationship between the untransformed TTP and $\log_{10}$(cfu) for this study.

All model fittings were conducted in the R statistical software environment (version 3.0.2). Linear regression analyses were carried out using the lm function, and R^2 was used to assess goodness of fit by standard methodology. Other non-linear models were also fitted, using the nls function, with the Akaike Information Criterion (AIC) used to assess the quality of the statistical model. Model selection was then based on the smallest AIC value. Negative cultures were handled by setting cfu values to 1 and TTP measurements to 1008 hours, which is the longest time MGIT will signal positive. Only time points where both TTP and cfu were measured were included in the analysis.

A conversion formula to translate TTP and cfu was created from half of the HIGHRIF1 dataset (the training set), based on the values from the Gompertz model (outlined below) for the changing gradients. This formula was then tested on the second half of the HIGHRIF1 dataset (the testing set).

RESULTS

Analysis of the combined data set

In this analysis we initially made the assumption that the dose of rifampicin did not affect the proportion of non-culturable cells detected. Bacterial load as reflected in TTP (hours) and colony forming units (cfu) determined on solid medium were analysed for each visit. TTP was plotted against $\log_{10}$(cfu) showing a negative correlation. This pattern was consistent on all 14 days of the study. These linear regression analyses are illustrated in Figure 1 (a)-(j) and the numeric estimates for the absolute values of the gradients and the y-intercepts are tabulated in Table 1.

There is a trend for the gradient of the regression line and y-intercept to increase as treatment progresses. To demonstrate the changing relationship, all of the regression lines were plotted together on a single graph (Figure 2) where the colours represent different days of treatment from dark blue (baseline) through to yellow (day 14). The steepness of the slope increases, particularly over the first few days (see Table 1). An analysis of covariance (ANCOVA) showed that this change in gradients was statistically significant with a p-value of 0.0002. This can be illustrated by the example, if two samples with a cfu count of 10^4 tested in MGIT, one at baseline and the other at day 14, they would take 150 and 280 hours, respectively, to signal positive. If all of the bacterial cells were being detected this relationship should not change.

In order to find a parametric form to describe how the gradients and y-intercepts change with each visit, we fitted a variety of functions to the changing profile: a

simple straight-line model, a segmented straight-line model, a Gompertz function and other exponential models. The results of the two best fitting functions, the simple straight-line model, $(m_1 t + c_1)\log(cfu) + (m_2 t + c_2)$, and the Gompertz function, $\left(i_1 e^{j_1 e^{k_1 t}}\right)\log(cfu) + \left(i_2 e^{j_2 e^{k_2 t}}\right)$, are discussed, where t is the number of days on treatment.

The two models are illustrated in Figure 3, where the red line shows the straight-line model and the black curve shows the Gompertz model. Numeric estimates for the parameter values and AIC values for both models are tabulated in Table 2, where the parameters were estimated using half of the HIGHRIF1 data (the training dataset). Based on these analyses, the Gompertz model was selected as the best model considered.

A similar pattern was observed in the OEBA data set, with the gradient of the regression line and y-intercept increasing as treatment progressed (linear regression analyses are illustrated in Figure S1 in the supplementary material). The increase in gradient, however, is not as steep as for the HIGHRIF1 data. A straight-line model and a Gompertz function were fitted in order to compare to the HIGHRIF1 data. These models are illustrated in Figure 4, where the red line shows the straight-line model and the black curve shows the Gompertz model. Numeric estimates for the parameter values and AIC values for both models are tabulated in Table 3. Based on these analyses, the Gompertz model was selected as the best model.

Conversion formula

An equation relating $\log_{10}$(cfu) and MGIT TTP was developed based on the Gompertz model, $TTP = \left(i_1 e^{j_1 e^{k_1 t}}\right) \log(cfu) + \left(i_2 e^{j_2 e^{k_2 t}}\right)$.

$\log(cfu) = \frac{TTP - \left(i_2 e^{j_2 e^{k_2 t}}\right).}{\left(i_1 e^{j_1 e^{k_1 t}}\right)}$, where t denotes days on treatment.

Using parameter estimates derived from the HIGHRIF1 training dataset, the following formula is constructed

$$\log(cfu) = \frac{TTP - \left(562.318 e^{-0.789 e^{-0.195 t}}\right)}{-64.111 e^{-1.002 e^{-0.248 t}}}.$$

In order to test this conversion formula, we validated against the HIGHRIF1 testing dataset. The actual cfu values from the testing dataset and the predicted cfu counts using the conversion formula were plotted in Figure 5.
Bias and imprecision calculations for the conversion formula, which are expressed as median percentage error (MPE) and median absolute percentage error (MAPE) (see supplementary material for formulae), were calculated, with MPE ranging from -3.5% to 7.1%, and MAPE ranging from 6.9% to 17.1%. Table S1 in the supplementary material tabulates MPE and MAPE for each visit.

Differences in treatment arms

We completed analyses on the gradient estimates for the whole HIGHRIF1 dataset over the first 7 days, analysing the treatment arm cohorts separately.

Only the first 7 days are analysed because standard HRZE treatment is administered after this time. We used simple linear regression, as a straight-line model was found to fit best when only modelling the first 7 days of treatment. In all cases, we find an increase in the magnitude of gradient over time, i.e. the same general pattern as with the pooled data, but this differs between treatment arms. Results are illustrated in Figure 6 and the numeric estimates are tabulated in Table 4. The slope of the straight line between the gradient estimates increases with dose.

DISCUSSION

The aim of this study was to relate the time to positivity (TTP) in MGIT to the number of colony forming units. By using sequential samples examined by both methodologies daily over two weeks we were able to explore how the relationship between these two cell types changed over time and in response to treatment. We found that if two samples had the same cfu count, the sample taken at a later visit would take longer to signal positive in MGIT.

An important observation is that the magnitude of the regression line gradient increases in the first few days of treatment. This increase in magnitude of gradient then slows for the remainder of the treatment. Although there is always a negative relationship between cfu and TTP throughout the 14 days of treatment, the time it takes for a sample with identical cfus to signal positive in MGIT changes during the treatment, with higher TTP values later in treatment. This pattern is also shown with contour plots, which show an upward trend in

TTP over time for constant cfu values (data not shown). One explanation of this is that MGIT is counting an extra sub-population of cells and this sub-population decreases in number over treatment, at a faster rate with higher dose of rifampicin. Alternative explanations include a change in lag phase or as a result of sub-lethal damage by rifampicin. The increase in gradient of the regression line relating TTP and cfu slows after the initial few days of treatment, meaning that the disparity between cfus and total cells contributing to a positive signal in MGIT is reducing. This would suggest that this extra cell population is being reduced rapidly by rifampicin. Alternatively it may be due to mycobacterial cell damages changing their ability to grow on liquid or solid media. Although a post antibiotic effect is an alternative explanation this is likely to be too short to have has this degree of effect.[19] An argument against a change in lag phase or post-antibiotic effect is that we found a similar pattern of increasing gradient over treatment emerges when we analyse data from the OEBA study that uses standard HRZE treatment. The gradient increases over time for these data, as in the HIGHRIF1 data, but here the increase is less rapid, with similar results to the control case for the HIGHRIF1 dataset.

When we analyse the treatment cohorts separately, we find that as the rifampicin dose increases, the slope of the regression line between the gradient estimates also increases. This seems to support the idea that rifampicin, particularly at higher doses, is able to kill, or at least damage, the population of cells that are detected by MGIT, but missed by colony counting.[20,21] This finding suggests that, although we show the conversion formula between cfu and TTP

appears to provide high predictability, future conversion formulae should be derived separately for each treatment regimen.

Short duration monotherapy studies have an important role in the early evaluation of anti-tuberculosis drugs and dosing. A frequent observation is that isoniazid has a very potent effect over the first two days, and that activity of another drug combinations with isoniazid cannot be detected.[17,22] This has led to the assumption that isoniazid is responsible for most of the killing early in tuberculosis chemotherapy and that rifampicin is responsible for sterilizing, i.e., killing "dormant" cells. The increased clearance of these "dormant" bacteria by rifampicin that this study suggests indicates that rifampicin may also be responsible for a large early reduction in bacterial load. The data reported in this paper suggest that higher doses of rifampicin may help to eradicate many non-culturable cells in the early days of treatment and support treatment shortening.

We have been able to use these data to formulate a tool to translate TTP into cfu. Considering the variability in the colony counting methodology, the equation seems to predict cfu count well, with MAPE values between 6.9%-17.1%. This shows acceptable predictive performance.[23] In the future, this approach should be used to derive distinct formulae for patients treated by different therapeutic regimens. Once appropriately validated, these formulae would significantly reduce the cost of performing early phase monotherapy and combination studies by removing the need for doing cfu counting on solid media.

In order to test whether our time-dependent formula converting TTP into cfu was an improvement on a simple straight line relationship that does not change over time, we calculated least squares estimates of each predicted $\log_{10}$(cfu) against the actual median value of the testing HIGHRIF1 dataset. We found that the straight-line relationship that did not change over time had larger least squares estimates than our time-dependent formula outlined earlier. We therefore conclude that a time-dependent conversion formula could be considered superior to a formula that does not take into account that the relationship between TTP and cfu changes over time.

When fitting regression lines to each visit to find the relationship between TTP and $\log_{10}$(cfu), the goodness of fit was measured by R^2 with values ranging from 0.3-0.73 (see Table 1). The high variability in accuracy of these counting methods due to variability in the number of organisms in sputum samples on the same day and the tendency of organisms to clump, means that finding close fitting relationships is often difficult and this accounts for some of these low R^2 values. As we have shown, there are differences in the relationship between TTP and cfu when different therapies are administered. This means that the conversion formula derived for this combined HIGHRIF1 dataset may not be as accurate as if it were derived separately for each cohort of patients receiving different treatments. With larger patient cohorts available, this method should be used to calculate distinct conversion formulae for different regimens.

In conclusion, we have demonstrated a population of mycobacterial cells that do not grow on solid medium. Increasing doses of rifampicin differentially kill this

group of organisms. If it is true that this sub-population is representative of dormant cells this could have important implications for treatment duration.

FUNDING

This work was supported by EDCTP who fund the PanACEA consortium (IP.2007.32011.011, IP.2007.32011.012, IP.2007.32011.013) and PreDiCT-TB consortium (IMI Joint undertaking grant agreement number 115337, resources of which are composed of financial contribution from the European Union's Seventh Framework Programme (FP7/2007-2013) and EFPIA companies' in kind contribution.

TRANSPARANCY DECLARATIONS

All authors: none to declare.

Contribution of authors

Preparation of manuscript - first draft: RB, SHG. Further contributions: MJB, RA, RD, AD, CM, NH, NN, AK, BM, PPJP, AR, GP.

Development of model: RB, SHG.

Data Analysis: RB, SHG, PPJP, RA, NH.

Collection of data: MJB, RA, AD, CM, NH, NN, AK, BM, AR, GP.

REFERENCES

1. Ginsberg AM. Tuberculosis drug development: Progress, challenges, and the road ahead. *Tuberculosis* 2010; **90**: 162–7.

2. Chao MC, Rubin EJ. Letting sleeping dos lie: does dormancy play a role in tuberculosis? *Annu Rev Microbiol* 2010; **64**: 293–311.

3. Wayne LG, Hayes LG. An in vitro model for sequential study of shiftdown of Mycobacterium tuberculosis through two stages of nonreplicating persistence. *Infect Immun* 1996; **64**: 2062–9.

4. Shleeva MO, Kudykina YK, Vostroknutova GN *et al*. Dormant ovoid cells of Mycobacterium tuberculosis are formed in response to gradual external acidification. *Tuberculosis (Edinb)* 2011; **91**: 146–54.

5. Hu Y, Coates ARM, Mitchison DA. Comparison of the sterilising activities of the nitroimidazopyran PA-824 and moxifloxacin against persisting Mycobacterium tuberculosis. *Int J Tuberc Lung Dis* 2008; **12**: 69–73.

6. Jindani A, Aber VR, Edwards EA *et al*. The early bactericidal activity of drugs in patients with pulmonary tuberculosis. *Am Rev Respir Dis* 1980; **121**: 939–49.

7. Grosset J, Almeida D, Converse PJ *et al.* Modeling early bactericidal activity in murine tuberculosis provides insights into the activity of isoniazid and pyrazinamide. *Proc Natl Acad Sci USA* 2012; **109**: 15001–5.

8. Garton NJ, Christensen H, Minnikin DE *et al*. Intracellular lipophilic inclusions of mycobacteria in vitro and in sputum. *Microbiology (Reading, Engl)* 2002; **148**: 2951–8.

9. Shleeva MO, Bagramyan K, Telkov MV *et al.* Formation and resuscitation of 'non-culturable' cells of Rhodococcus rhodochrous and Mycobacterium tuberculosis in prolonged stationary phase. *Microbiology (Reading, Engl)* 2002; **148**: 1581–91.

10. Mukamolova GV, Kaprelyants AS, Young DI *et al*. A bacterial cytokine. *Proc Natl Acad Sci USA* 1998; **95**: 8916–21.

11. Deb C, Lee C-M, Dubey VS *et al.* A Novel In Vitro Multiple-Stress Dormancy Model for Mycobacterium tuberculosis Generates a Lipid-Loaded, Drug-Tolerant, Dormant Pathogen. *PLoS ONE* **4**: 15.

12. Loebel RO, Shorr E, Richardson HB. The Influence of Adverse Conditions upon the Respiratory Metabolism and Growth of Human Tubercle Bacilli. *J Bacteriol* 1933; **26**: 167–200.

13. Wayne LG. Growth of Mycobacterium tuberculosis from resected specimens under various atmospheric conditions. *Am Rev Tuberc* 1954; **70**: 910–1.

14. Davies AP, Dhillon AP, Young M *et al*. Resuscitation-promoting factors are expressed in Mycobacterium tuberculosis-infected human tissue. *Tuberculosis* 2008; **88**: 462–8.

15. Mukamolova GV, Turapov O, Malkin J *et al*. Resuscitation-promoting Factors Reveal an Occult Population of Tubercle Bacilli in Sputum. *Am J Respir Crit Care Med* 2010; **181**: 174–80.

16. Diacon AH, Maritz JS, Venter A, *et al* Time to liquid culture positivity can substitute for colony counting on agar plates in early bactericidal activity studies of antituberculosis agents. *Clin Microbiol Infect* 2012; **18**: 711–7.

17. Gillespie SH. Early bactericidal activity of a moxifloxacin and isoniazid combination in smear-positive pulmonary tuberculosis. *J Antimicrob Chemoth* 2005; **56**: 1169–71.

18. Perrin FMR, Woodward N, Phillips PPJ *et al.* Radiological cavitation, sputum mycobacterial load and treatment response in pulmonary tuberculosis. 2010; **14**: 1596–602.

19. Thorburn CE, Molesworth SJ, Sutherland R *et al*. Postantibiotic and post-beta-lactamase inhibitor effects

of amoxicillin plus clavulanate. *Antimicrob Agents Chemother* 1996; **40**: 2796–801.

20. Gumbo T, Louie A, Deziel MR *et al.* Concentration-Dependent Mycobacterium tuberculosis Killing and Prevention of Resistance by Rifampin. *Antimicrob Agents Chemother* 2007; **51**: 3781–8.

21. de Steenwinkel JEM, Aarnoutse RE, de Knegt GJ *et al.* Optimization of the Rifampin Dosage to Improve the Therapeutic Efficacy in Tuberculosis Treatment, using a Murine Model. *Am J Respir Crit Care Med* 2013; **187**: 1127-34.

22. Jindani A, Doré CJ, Mitchison DA. Bactericidal and sterilizing activities of antituberculosis drugs during the first 14 days. *Am J Respir Crit Care Med* 2003; **167**: 1348–54.

23. David OJ, Johnston A. Limited sampling strategies for estimating cyclosporin area under the concentration-time curve: review of current algorithms. *Ther Drug Monit* 2001; **23**: 100–14.

FIGURE LEGENDS

Figure 1: Plots of MGIT TTP (hours) against Log_{10} of cfu for each time point in the PanACEA HIGHRIF1 study, baseline through to day 14 with regression lines fitted. The days are represented (a) = day 0 (61 observations), (b) = day 1 (60 observations), (c) = day 2 (58 observations), (d)= day 3 (55 observations), (e)= day 4 (59 observations), (f)= day 5 (59 observations), (g)= day 6 (54 observations), (h) = day 7 (53 observations), (i) = day 9 (46 observations), (j)= day 14 (37 observations).

Figure 2: Regression line fits for the HIGHRIF1 data, for all time points. Included colour table shows which line corresponds to which time point. Baseline is at the left of the colour table, day 14 at the right.

Figure 3: HIGHRIF1 training data plots of the absolute value of the gradients of each time point (a), and y-intercepts for each time point (b), with estimated fitted regression line and Gompertz curve overlaid.

Figure 4: OEBA data plots of the absolute value of the gradients of each time point (a) and y-intercepts for each time point (b) with fitted regression line and Gompertz curve overlaid.

Figure 5: Log10(cfu) values are plotted (grey circles) for all 68 patients in the HIGHRIF1 testing dataset during treatment. The asterisks show the median values of the testing dataset at each time point. The line shows the predicted decline in cfu using the TTP values from the testing dataset, predicted using the conversion formula.

Figure 6: Plots of the gradient estimates during the first 7 days of treatment in different treatment arms of the HIGHRIF1 study, identified by RIF dose, with (a) control arm, (b) 20 mg, (c) 25 mg, (d) 30 mg, (e) 35 mg. Fitted straight lines are shown in red.

TABLE LEGENDS

Table 1: Linear regression fitted estimates with R^2. Note that all estimates were fitted with p-values < 0.001.

Table 2: Fitted values for the straight line and Gompertz models for the HIGHRIF1 training dataset. Note that in both models, all estimates were fitted with p-values < 0.01.

Table 3: Fitted values for the straight line and Gompertz models for the OEBA data. Note that in both models, all estimates were fitted with p-values < 0.01.

Table 4: Parameter estimates for the linear regression analyses conducted in each treatment arm. Straight lines are fitted to the absolute value of the gradients and y-intercepts as functions of time.

FIGURES

Figure 1

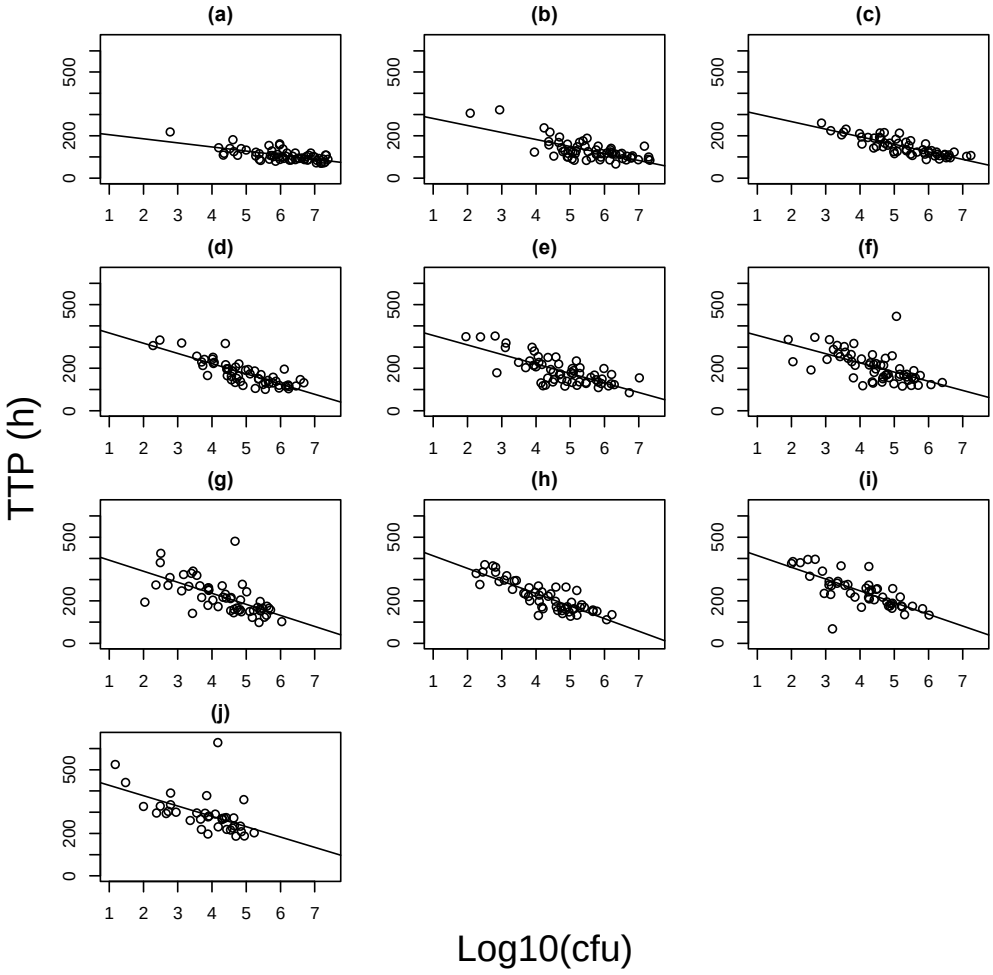

Figure 2

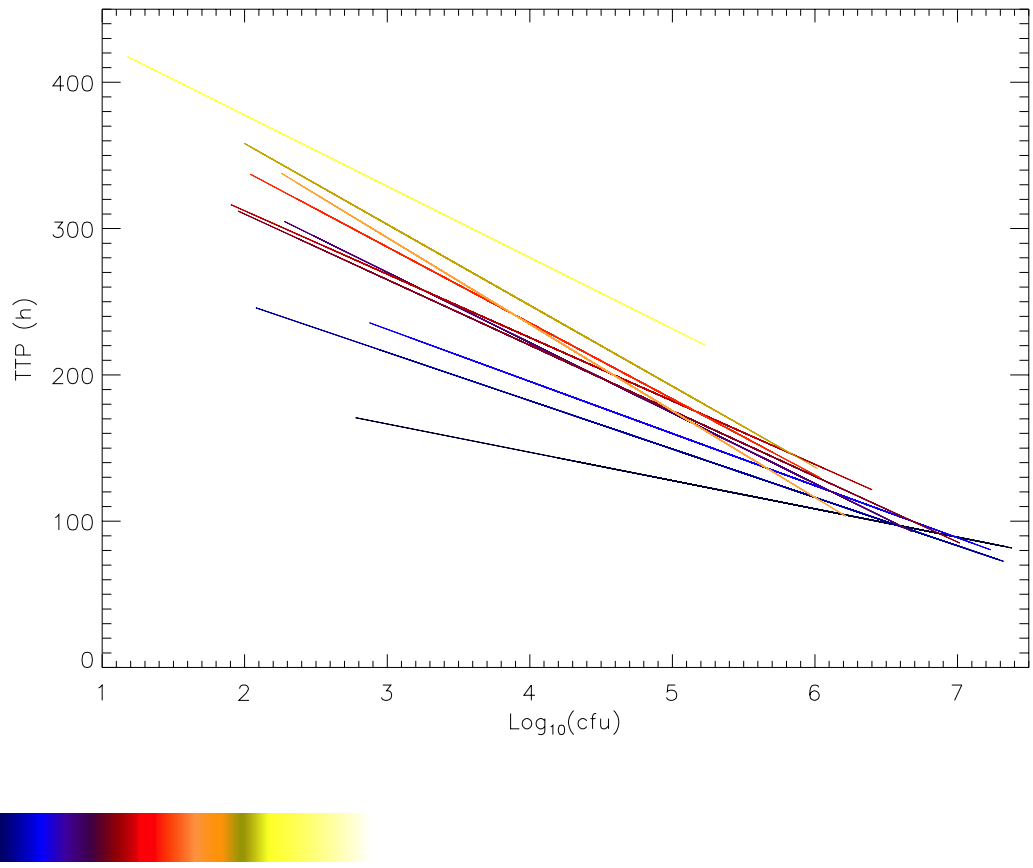

Figure 3

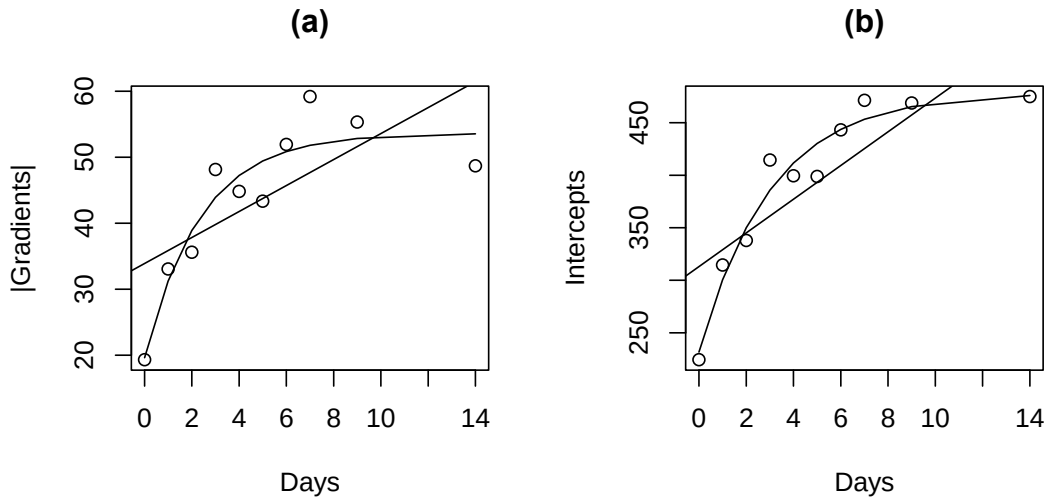
(a)
|Gradients|
20
30
40
50
60
0
2
4
6
8
10
14
Days
(b)
Intercepts
250
350
450
0
2
4
6
8
10
14
Days

Figure 4

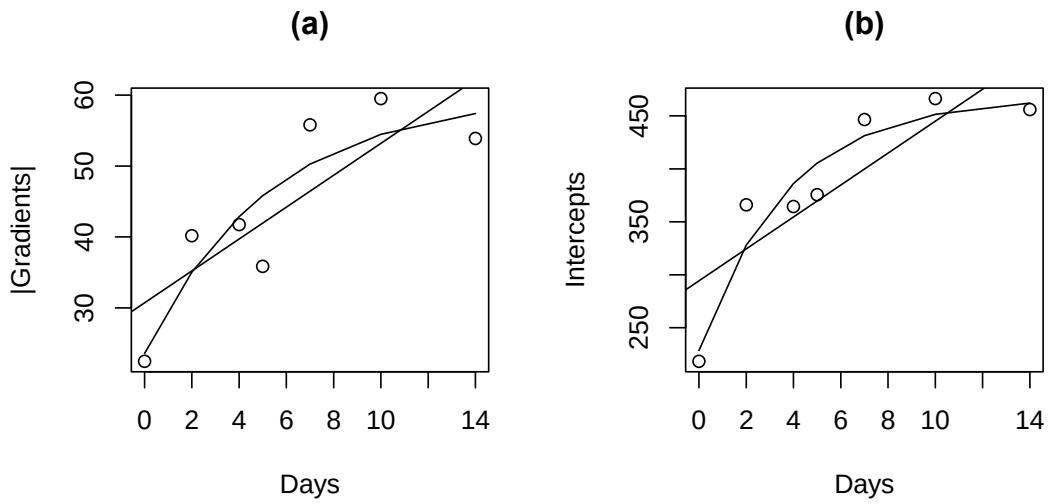
(a)
|Gradients|
30
40
50
60
0
2
4
6
8
10
14
Days
(b)
Intercepts
250
350
450
0
2
4
6
8
10
14
Days

Figure 5

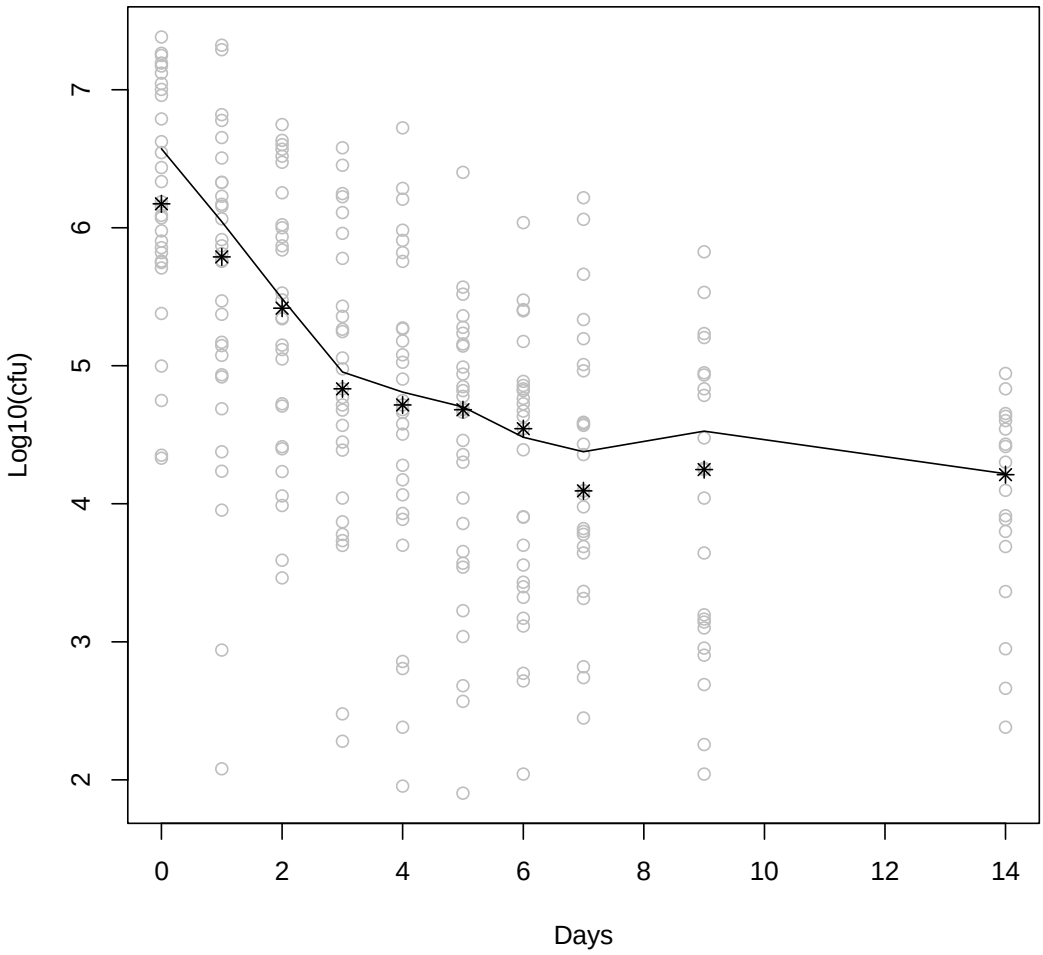

Figure 6

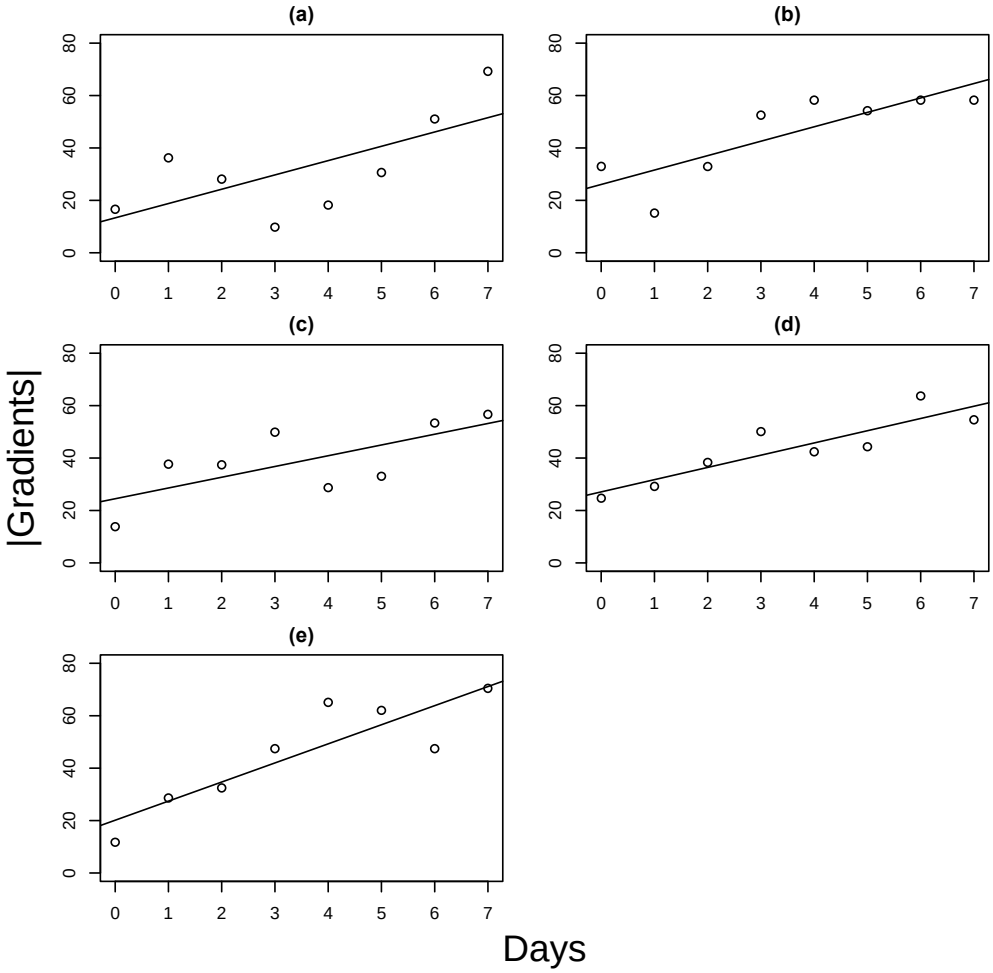

Tables

Table 1

	Absolute value of the gradient estimate	y-intercept estimate	R^2
Baseline	19.33	224.42	0.46
Day 1	33.05	314.57	0.49
Day 2	35.61	337.97	0.73
Day 3	48.13	414.53	0.67
Day 4	44.81	399.51	0.54
Day 5	43.33	398.83	0.37
Day 6	51.93	443.23	0.41
Day 7	59.18	471.37	0.72
Day 9	55.30	468.75	0.54
Day 14	48.67	474.91	0.30

Table 2

Straight-line Model: $\boldsymbol{TTP = (m_1 t + c_1)\log(cfu) + (m_2 t + c_2)}$					
$\boldsymbol{m_1}$	$\boldsymbol{c_1}$	$\boldsymbol{m_2}$	$\boldsymbol{c_2}$		**AIC**
-2.09	-33.76	16.57	315.51		2892.67
Gompertz Model: $\boldsymbol{TTP = \left(i_1 e^{j_1 e^{k_1 t}}\right)\log(cfu) + \left(i_2 e^{j_2 e^{k_2 t}}\right)}$					
$\boldsymbol{i_1}$	$\boldsymbol{j_1}$	$\boldsymbol{k_1}$	$\boldsymbol{i_2}$	$\boldsymbol{j_2}$	$\boldsymbol{k_2}$	**AIC**
-64.11	-1.00	-0.25	562.32	-0.79	-0.20	2691.70

Table 3

Straight-line Model: $TTP = (m_1 t + c_1)\log(cfu) + (m_2 t + c_2)$					
m_1	c_1	m_2	c_2		**AIC**
-0.51	-41.38	6.78	346.71		1396.69
Gompertz Model: $TTP = \left(i_1 e^{j_1 e^{k_1 t}}\right)\log(cfu) + \left(i_2 e^{j_2 e^{k_2 t}}\right)$					
i_1	j_1	k_1	i_2	j_2	k_2	**AIC**
-54.85	-0.91	-0.43	449.89	-0.73	-0.50	1384.59

Table 4

Treatment group	$y = mx + c$		
	m	**c**	**R^2**
CONTROL	5.46	13.38	0.46
20mg/kg	5.50	26.06	0.69
25mg/kg	4.10	24.47	0.50
30mg/kg	7.28	20.16	0.77
35mg/kg	7.45	19.92	0.80